J. Physiol. (1971), **213**, *pp.* 31–53
With 10 *text-figures*
Printed in Great Britain

PREDICTION OF REPETITIVE FIRING BEHAVIOUR FROM VOLTAGE CLAMP DATA ON AN ISOLATED NEURONE SOMA

BY J. A. CONNOR* AND C. F. STEVENS

From the Department of Physiology and Biophysics, School of Medicine, University of Washington, Seattle, Washington 98105, U.S.A.

(*Received 27 May 1970*)

SUMMARY

1. Membrane parameters of an isolated neural cell body have been determined by voltage clamp analysis. Data are expressed as membrane ion-specific conductances, leak conductance, and capacitance.

2. Three ionic currents are present: Inward, I_I; and two operationally distinct outward currents, I_K and I_A. Both outward currents are apparently carried by potassium ions.

3. Hodgkin–Huxley-like equations were solved for the discharge of two sequential action potentials in response to a constant stimulus current. The digital computer solutions are compared with action potential data recorded from the investigated cell.

4. The computed and experimentally measured relationships between firing frequency and stimulus current intensity are compared and are linear over the same portion of the total frequency range.

5. Cell behaviour in the latter part of the interspike interval is dominated by the conductance g_A while g_{Na} and g_K largely determine the character of the action potential and the initial portion of the interspike interval.

6. Prehyperpolarization of the membrane activates g_A and the membrane response to depolarizing current differs markedly from the response elicited when no prehyperpolarization is imposed.

INTRODUCTION

The behaviour of gastropod neurone somas under voltage clamp conditions may be analysed in terms of three conductance mechanisms, g_I, g_K, and g_A, described in the first two papers of this series (Connor & Stevens,

* Present address: Department of Physiology and Biophysics, University of Illinois, Urbana, Illinois 61801, U.S.A.

1971*a*, *b*). The conductances g_I and g_K correspond to the g_{Na} and g_K in the analysis by Hodgkin & Huxley (1952), and exhibit qualitatively similar behaviour; the third conductance, g_A, has no counterpart in the Hodgkin–Huxley analysis, and seems not to have been explicitly recognized in previous experiments. Potassium ions appear to be the predominant current-carrying ion for g_A, its time constants are intermediate between those of g_I and g_K, and, because it becomes inactivated at above approximately -40 mV, its predominant role in neurone behaviour is limited to voltages in the subthreshold range.

The over-all goal of these investigations has been to provide an analysis of repetitive firing mechanisms in a specific preparation. In order to demonstrate that the properties of the conductances described in the preceding papers can indeed account for the repetitive firing exhibited by this neurone, it is necessary to produce Hodgkin–Huxley-like equations describing the voltage clamp behaviour of the cell and then show that the solution of these equations does indeed predict accurately the neurone behaviour under current clamp conditions. This programme is carried out in the present paper, and the analysis reveals that the three conductance mechanisms can account for the repetitive firing observed in these experiments. We conclude that, immediately following a spike, g_K dominates the neurone's behaviour, and as the increased g_K decays toward its resting values, g_A is activated and predominates during the middle and latter part of the interspike interval. The effect of the current through g_A is to counterbalance the currents through g_I and the stimulus current and thereby produce the typical membrane potential trajectory between action potentials.

The analysis presented here is carried out in two parts. In the first section of the paper, we shall present estimates for membrane capacitance, the conductance of leakage channels, and describe, in turn, the empirical equations for the behaviour under voltage clamp of g_I, g_A, and g_K. Because each of these conductances is to be represented as the product of two factors, it will be necessary to describe the kinetic behaviour of each factor in addition to its steady-state value as a function of membrane potential. Descriptions take the form of graphs which give the value of the parameter in question as a function of membrane potential. In the second section of the paper these equations are solved and the appropriate solutions are compared with the neurone's observed behaviour.

METHODS

We have attempted throughout to avoid pooling data from separate experiments, but rather to predict a cell's response to applied current from the voltage clamp analysis of only that cell. It is, however, difficult to obtain all the required data on

one cell, and we have thus formulated the equations and compared predicted and observed behaviour under current clamp conditions for only seven preparations. In this paper we have presented primarily data from a single cell, the one most completely analysed; the remaining six cells provide an entirely consistent picture.

To carry out a complete analysis over a full range of membrane potentials is very difficult indeed, and we have thus concentrated our efforts on the range of membrane potentials that are most important in repetitive firing, that is, between the potassium equilibrium potential (-63 mV) and the point at which the inward current mechanism g_I becomes strongly activated (-25 mV). Thus the equations to be presented are most accurate in that range; above -20 mV we have not been able to achieve equal accuracy for all parts of the description.

Because the currents which flow on a step change in membrane potential do not settle completely as quickly as one would like, it has not been possible to measure accurately the instantaneous voltage–current relationship over the entire relevant voltage range for these cells. The data available are consistent with the assumption that the instantaneous voltage–current relationship is linear and we will thus develop our formulation in terms of conductances rather than in permeabilities (Dodge & Frankenhaeuser, 1959; Frankenhaeuser & Huxley, 1964) or membrane current (Noble & Tsien, 1969*a*, *b*).

Thus the basic equation governing membrane behaviour is:

$$I(t) = C\frac{dV}{dt} + g_I(V - V_I) + g_K(V - V_K) + g_A(V - V_A) + g_L(V - V_L),$$

where I is the applied current, C the membrane capacitance, V the membrane potential, g_I, g_K, g_A the variable conductances with associated equilibrium potentials V_I, V_K, V_A. g_L is the leakage conductance and V_L its equilibrium potential. Equilibrium potentials were determined by the three methods described in the first paper of this series and are designated by the numbers given there (Connor & Stevens, 1971*a*).

Instead of describing the dependence of rate constants (our analogues of the Hodgkin–Huxley α's and β's) on voltage by empirical equations as Hodgkin & Huxley (1952) did, we have chosen to specify this information by piecewise linear approximations to the experimental data; the curves shown in Fig. 1, 2, 3, 4 and 5 are the ones used in calculations. Furthermore, we have described the temporal development of processes in terms of time constants, analogous to the Hodgkin & Huxley τ's, rather than rate constants. Because we distinguish between three types of voltage-sensitive channels, I, K and A, it is necessary to provide subscripts for the time constants to specify the channel involved; in addition, the behaviour of each channel will be described in terms of two underlying processes (analogous, for example, to the Hodgkin & Huxley m and h), denoted by the letters A and B, so a second subscript is required to indicate with which of these processes the time constant is associated. The convention adopted is to double subscript each time constant τ, with the first subscript specifying the underlying process, and the second subscript specifying the channel type. For example, τ_{BK} would be the time constant associated with the B-process of the potassium channels, and τ_{AA} would indicate the time constant associated with the A-process of the A channels. On some occasions, when the type of channel associated with a time constant is clear from the context, the second subscript will be suppressed.

Equations have been solved on a digital computer with a programme which uses a rectangular integration scheme. Time increments were changed over a large range to discover the values giving rise to errors in integration, and the values actually

used were always small compared to this. The accuracy of the integration programme has been checked by computing the solutions to equations whose solutions are tabulated.

RESULTS

SECTION 1

Membrane capacitance

Membrane capacitance was measured by injecting, under current clamp conditions, a constant hyperpolarizing current, and then measuring the initial voltage slope. Because g_I and g_K are constant under these circumstances, and g_A varies slowly if at all over the time required to make this observation, C (the soma capacitance) should be given by the ratio of applied current and the initial rate of change of voltage. The value of capacitance thus obtained for the exemplar cell is 14 nF (measurement uncertainty ± 2 nF), and values for other cells characteristically ranged between 12 and 35 nF. These values were found to be directly related to size of the cell. The exemplar cell was approximately spherical, with a diameter of approximately 250 μ.

Leakage conductance

Accurate values for the leakage conductance, g_L, were difficult to obtain because other conductances participate in the voltage–current relationships over a very wide range of membrane potentials; above -40 mV, steady-state inward and potassium currents are flowing, and below -40 mV g_A plays an important role. For very large hyperpolarizations, below membrane potentials of -100 mV (for example, see Ochs, 1967), the voltage–current relationship becomes very badly behaved because of precipitous and often unrepeatable or irreversible increases in membrane conductance. In the vicinity of -40 mV, g_A is almost completely inactivated, whereas g_I and g_K are not appreciably activated. Thus, we have taken the slope of the voltage–current relationship at this point to be the leakage conductance, and have used the intersection of the leakage conductance line with the voltage axis (point of zero current) as the leakage equilibrium potential. In the exemplar cell the leakage conductance measured in this way was estimated to be 0·049 μmhos with an equilibrium potential of -40 mV. Although this estimate is necessarily rather inaccurate, the total leakage current is generally sufficiently small to make imprecisions in estimates of g_L and V_L unimportant.

Description of g_I

In order to estimate the conductance g_I as a function of voltage and time it is necessary to separate the inward currents from the early phases of the outward potassium currents. This separation is probably best achieved when the potassium channels are blocked with TEA, a technique which seems to leave the inward current unaffected. Although the pharmacological separation has been used in some cases, in the exemplar cell the following alternative procedure was employed because it is too risky to change solutions. The delay in activation of the potassium conductance g_K is sufficiently long in most instances (see later Discussion) that the major part of the inward current flow is uncontaminated by I_K. Thus, by considering sufficiently short times, it is plausible to assume that the currents flowing consist of only inward current, and leakage current (at least for those situations in which g_A is essentially inactivated at the holding potential). It will be recalled from a preceding paper (Connor & Stevens, 1971*a*) that, after a brief delay, the inward current increases rapidly to a peak and then decays with what appears to be an exponential time course. The time constant of this decay was estimated from the steepest slope of the decay, and a point in time three of these time constants later was chosen as the steady-state value for inward currents. The conductance g_I was then estimated by subtracting leakage and any I_A or I_K present from the measured total currents, and then dividing by the difference between the membrane potential and the inward current equilibrium potential V_I. This equilibrium potential, estimated by methods (1) and (2), has a value of $+45$ mV.

The conductance g_I rises after a delay to a peak and then decays exponentially. It was found that an equation with the same form as that used by Hodgkin & Huxley for g_{Na} is adequate to describe the inward current mechanism in this membrane as well. Thus, g_I is given by

$$g_I(V, t) = \bar{g}_I A_I^3(V, t)\, B_I(V, t), \tag{1}$$

where $\bar{g}_I$ is the maximum conductance, $A_I(V, t)$ is the activation (analogous to the Hodgkin–Huxley m), and $B_I(V, t)$ is the inactivation (analogous to the Hodgkin–Huxley h). Activation and inactivation are described by the first-order differential equations

$$\left.\begin{aligned} \tau_{AI}(V)\,\frac{dA_I(V, t)}{dt} + A_I(V, t) &= A_I(V, \infty), \\ \tau_{BI}(V)\,\frac{dB_I(V, t)}{dt} + B_I(V, t) &= B_I(V, \infty), \end{aligned}\right\} \tag{2}$$

where τ_{AI} is the activation time constant and τ_{BI} the inactivation time constant. To describe g_I, it is then necessary to estimate $\bar{g}_I$, τ_{AI}, τ_{BI}, $A_I(V, \infty)$ and $B_I(V, \infty)$ from the experimental data.

To estimate the inactivation time constant $\tau_{BI}(V)$, semi-logarithmic plots for the approach of empirically determined g_I toward its steady-state values were prepared for a range of clamping voltages. Straight lines were fitted to the experimental points by eye, and the time constants $\tau_{BI}(V)$ were determined. The values for the time constant of decay determined

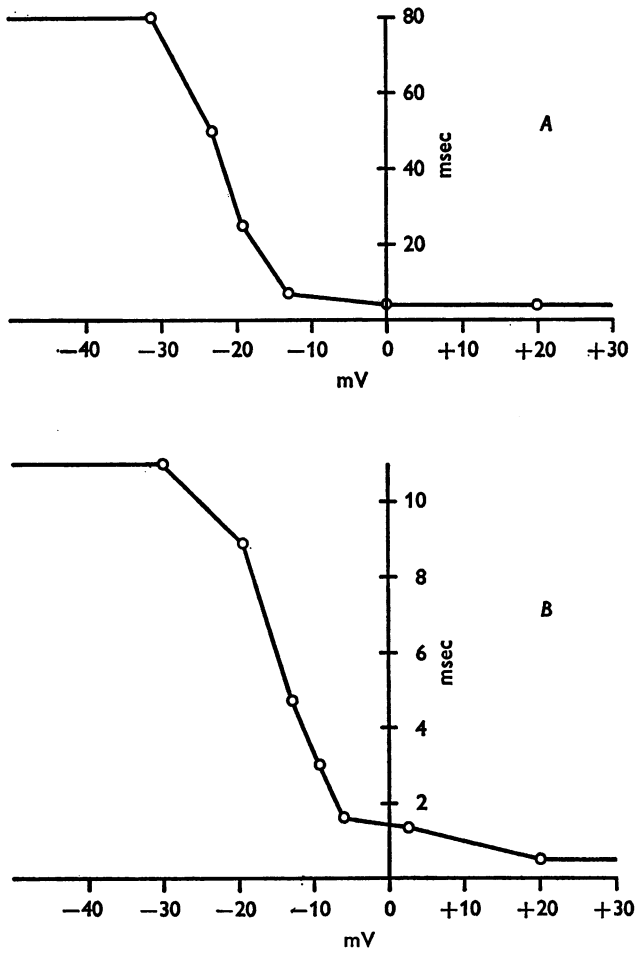

Fig. 1. *A*. Ordinate: inactivation time constant, τ_{BI}, for inward conductance *vs.* membrane voltage (abscissa). Measurement procedure is described in text. The straight line interpolation between data points shown in the figure was used in computing solutions to the membrane equation and is employed in all of the Figures of this section. *B*. Activation time constant, τ_{AI}, for inward conductance (abscissa) *vs.* membrane voltage (ordinate). Temp. 5° C.

in this way were compared with the preliminary estimates, and where the more precisely determined time constants gave a significantly different value for the steady-state current (at three time constants from the start of decay) the process was repeated. The final estimates of $\tau_{BI}(V)$ are shown in Fig. 1.

If the membrane potential is held at various levels and then stepped to some fixed level, differences in $g_I(V,t)$ that are measured reflect the steady-state values of inactivation at the holding potential. Although a more complicated procedure is required for the most precise estimates of $B_I(V,\infty)$, it is adequate for the present purposes to estimate this function by plotting peak conductances as a function of holding potential, and normalizing the largest values to one. This procedure yields the steady state inactivation curve given in Fig. 2.

Once the inactivation time constants and steady-state values of inactivation have been determined as described above, it is possible to estimate $A_I(V,\infty)$ from the observed values of g_I which result for a series of clamps from a fixed holding potential to a variable clamping potential. As long as activation occurs rapidly compared to inactivation, the following equation holds for the decaying phase of the conductance curves.

$$g_I(V,t) = \bar{g}_I A_I^3(V,\infty) B_I(V,t). \tag{3}$$

Since $B_I(V,t)$ is known, the decaying phase of $g_I(V,t)$ may be extrapolated back to time zero (the time membrane potential was stepped from its holding value to the clamped potential), and the quantity $\bar{g}_I A^3(V,\infty)$ may be found. The maximum value of this quantity is taken to be $\bar{g}_1$, and $A^3(V,\infty)$ is thus determined. A value of 21 μmhos was the $\bar{g}_I$ for the exemplar cell, and the steady-state values of activation $A_I^3(V,\infty)$ are shown in Fig. 2.

The rising phase of g_I is generally too seriously contaminated with the capacity transient current to permit a meaningful determination of the activation time constant τ_{AI}. Thus, the value for the activation time constant required at each clamping voltage to produce the observed time of peak conductance was determined. These estimates of $\tau_{AI}(V)$ are given in Fig. 1.

Description of g_A

Determination of the equilibrium potential for I_A has been described in the preceding paper. Value for the exemplar cell is -63 mV, and other experiments have yielded values between -55 and -68 mV.

The description of $g_A(V,t)$ is obtained by first considering the voltage range where this conductance alone is active, and later extending the description to more depolarized values where it is necessary to separate the effects of g_A and g_K. For potentials more negative than -35 mV, then,

$g_A(V, t)$ is found by subtracting the leakage currents from the total currents and dividing by the difference between membrane potential and the equilibrium potential, V_A. The following equation was found to describe g_A.

$$g_A(V, t) = \bar{g}_A A_A^4(V, t) B_A(V, t), \tag{4}$$

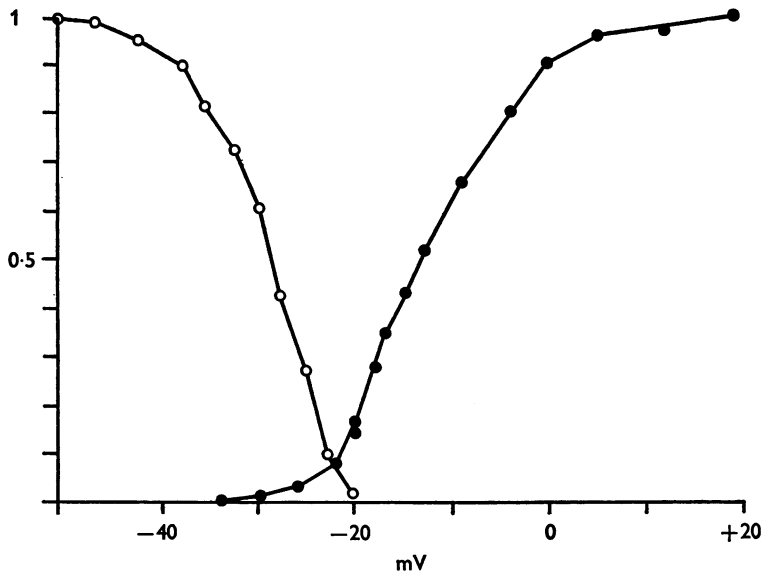

Fig. 2. Ordinate: inactivation, $B_I(V, \infty)$, (open circles) and activation, $A_I^3(V, \infty)$, (filled circles) characteristics for inward conductance plotted against membrane potential (abscissa). Each set has been normalized to its maximum value on the voltage range studied. Note that curves overlap between -30 and -20 mV.

where $\bar{g}_A$ is the peak conductance, A_A is the activation term, and B_A is the inactivation term. The activation and inactivation terms are described by the first-order differential equations

$$\left.\begin{aligned} \tau_{AA}(V)\frac{dA_A(V, t)}{dt} + A_A(V, t) &= A_A(V, \infty), \\ \tau_{BA}(V)\frac{dB_A(V, t)}{dt} + B_A(V, t) &= B_A(V, \infty), \end{aligned}\right\} \tag{5}$$

where τ_{AA} is the time constant for activation, and $A_A(V, \infty)$ is the steady-state value; similarly, τ_{BA} is the inactivation time constant, and $B_A(V, \infty)$ is the steady-state value of inactivation. As before then, two time constants, and steady-state values for activation and inactivation must be determined from the experimental data.

Appropriate manipulation of eqns. (4) and (5) reveals that the activation and inactivation time constants were estimated in the previous analysis of the currents I_A (Connor & Stevens, 1971*b*); these time constants appear in eqn. (1) of that paper. For the exemplar cell $\tau_{AA} = 12$ msec and $\tau_{BA} = 235$ msec. Unlike the activation and inactivation time constants for other processes, τ_{AA} and τ_{BA} do not appear to depend upon membrane potential.

The steady-state values for inactivation of this process may be determined by measuring the peak value of g_A that results when the membrane is clamped from various holding potentials to a fixed clamping potential.

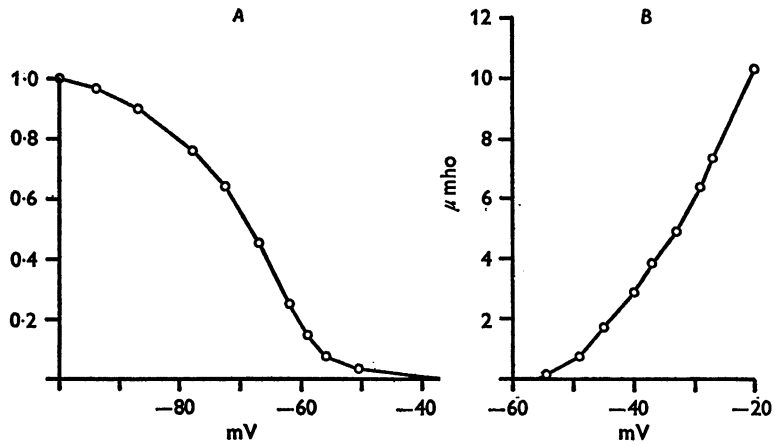

Fig. 3. *A*. Ordinate: normalized inactivation characteristics of g_A, $B_A(V, \infty)$. Abscissa: membrane potential. *B*. Ordinate: activation characteristics of g_A, $\bar{g}_A A_A^4(V, \infty)$. Abscissa: membrane potential.

This determination yields $B_A(V, \infty)$ up to a multiplicative constant, and by taking the maximum value of g_A as unity, the inactivation curve may be normalized to values between one and zero. The steady-state inactivation $B_A(V, \infty)$ for the exemplar cell is shown in Fig. 3*A*. The curves obtained from other cells are, within the range of experimental error, essentially the same.

To determine the activation curve for g_A, the following procedure was used: membrane voltage was held at a given hyperpolarized value, −88 mV in the exemplar cell; voltage was then stepped to a less negative value and the resulting transient current measured. This was repeated for a family of clamping voltages ranging from −60 to −30 mV. After correcting total current for leakage current, the conductance $g_A(V, t)$ was computed. The equation

$$g_A(V, t) \approx \bar{g}_A A_A^4(V, \infty) B_A(V, t) \quad (t > 50 \text{ msec})$$

holds for time greater than 50 msec with an error of less than 5%. The activation term is then found by extrapolating the plot of $g_A(V, t)$ back to time zero. The value of the intercept divided by the previously determined value of $B_A(V, \infty)$ at the holding potential used gives an estimate of $\bar{g}_A A_A^4(V, \infty)$. It has proved impractical to separate $\bar{g}_A$ and A_A, and consequently, in Fig. 3*B*, the steady-state values of $\bar{g}_A A^4(V, \infty)$ are plotted as a function of voltage for the exemplar cell. Other preparations yield essentially similar plots.

For clamping voltages more positive than -30 mV, the I_K and I_A currents were separated by the subtraction procedure described in the preceding paper (see Connor & Stevens, 1971*b*; Fig. 12). The I_A currents thus obtained are used to extend the steady-state activation curve to more polarized values as shown in Fig. 3*B*. For membrane potentials more positive than those shown in Fig. 3*B*, the I_K currents develop more rapidly and become very large, and consequently the separation of the two processes becomes inaccurate. As is apparent from Fig. 3*B*, the A-process activation has not yet reached asymptote for the most positive membrane potentials for which measurements can be accurately made; it is for this reason that $\bar{g}_A$ and $A_A(V, \infty)$ are not estimated separately.

Description of g_K

The equilibrium potential for I_K determined by methods (2) and (3) was -60 mV for the exemplar cell. Because g_A is inactivated for membrane potentials more positive than -40 mV, by holding the cell at this potential value and clamping to more depolarized levels, it was possible to obtain currents uncontaminated by I_A. Furthermore, because the I_I transients are so much more rapid than the I_K currents for voltages above -20 mV, the inward currents can usually be eliminated by ignoring the shorter times. In most cases then, g_K could be estimated by merely subtracting the leakage current from the total currents (ignoring the time during which inward currents were flowing), and dividing by the difference between membrane potential and equilibrium potential. In that voltage range where steady-state inward currents flow (see Fig. 2), it was, of course, necessary to subtract the steady inward current from the total current in order to separate I_K.

Because our main concern has been with predicting the voltage trajectory during the interspike interval, in many instances we used the following procedure to study g_K: (1) the membrane was clamped to a holding potential, (2) the clamp was released and a spike was initiated, and (3) the clamp was re-instituted at a clamping potential during the downswing of the spike. In this situation the decay of potassium conductance after a normal spike could be investigated. If the prespike membrane potential

was held at -40 mV or above, only leakage current and I_K flowed during the post-spike period because g_A was inactivated. For prespike holding voltages more negative than -40 mV, g_A became a factor and an appropriate correction for the presence of I_A would have to be made. The conductance g_K after a spike was then determined by dividing I_K by the difference between the post-spike clamping potential and V_K.

A Hodgkin–Huxley-like description of g_K was attempted, but the third- or fourth-power dependence of g_K on a process satisfying a first-order differential equation was found not sufficiently accurate. The following equations were, however, found to be adequate:

$$g_K(V,t) = \bar{g}_K A_K^2(V,t) B_K(V,t), \tag{6}$$

$$\tau_{AK}(V)\frac{dA_K(V,t)}{dt} + A_K(V,t) = A_K(V,\infty),$$

$$\tau_{BK}(V)\frac{dB_K(V,t)}{dt} + B_K(V,t) = B_K(V,\infty). \tag{7}$$

As before, the time constants τ_{AK} and τ_{BK}, and the steady-state values $\bar{g}_K A_K^2(V,\infty)$ and $B_K(V,\infty)$ must be found. It must be emphasized that, although these equations have been written in a form like that used in the preceding descriptions of g_I and g_A, B_K has a somewhat different significance. Because the time constant of potassium inactivation was long compared to the times of interest, potassium inactivation is *not* included in eqns. (6) and (7), and so B_K is *not*, as in the preceding equations, an inactivation term. Rather, B_K is a second component of activation and the steady-state values of A_K and B_K both increase toward one as the membrane is depolarized from the resting potential ($-$ 40 mV).

During an action potential g_K increases to quite large values, and, by clamping the membrane potential to some specified level immediately after an action potential, the return of g_K toward its steady-state values may be studied. According to eqns. (6) and (7), g_K after a spike should have the form

$$g_K(V,t) = \bar{g}_K([A_0 - A(V,\infty)]\exp(-t/\tau_{AK}) + A(V,\infty))^2([B_0 - B(V,\infty)]\exp(-t/\tau_{BK}) + B(V,\infty))$$

A_0 and B_0 are the values of these parameters which obtain immediately after the spike. For membrane potentials more negative than about -30 mV, $A_K(V,\infty)$ is found to be near zero, and the decay of potassium conductance following an action potential has the form

$$g_K(V,t) = \bar{g}_K A_0^2 \exp(-2t/\tau_{AK}) \times([B_0 - B_K(V,\infty)]\exp(-t/\tau_{BK}) + B_K(V,\infty)) \tag{8}$$

This equation is the sum of two exponentials, and, because the time constants τ_{AK} and τ_{BK} are sufficiently different it is not difficult to separate g_K into the sum of two components when the conductance or current is

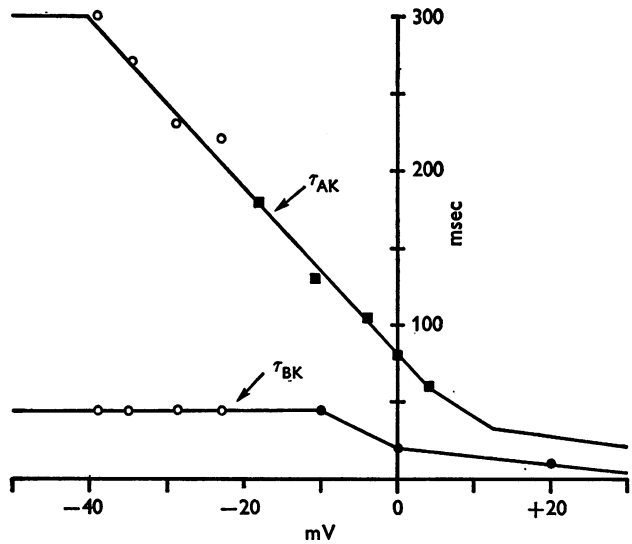

Fig. 4. Abscissa: time constants for outward conductance, g_K, plotted against membrane potential (ordinate). Open circles were derived from post-spike clamp data (see text).

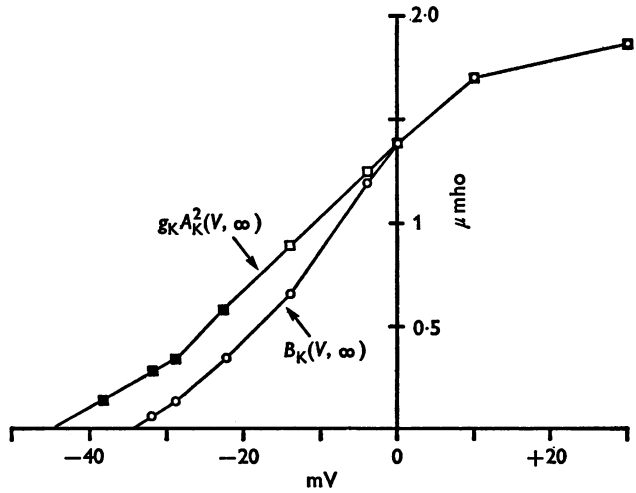

Fig. 5. $\bar{g}_K A_K^2$ (V, ∞), in μmhos, and B_K (V, ∞), unitless, plotted as a function of membrane potential. Filled squares were derived from post-spike clamp data. As the form of B_K (V, ∞) and $\bar{g}_K A_K^2$ (V, ∞) are the same for membrane potentials more positive than 0 mV, B_K (V, ∞) has been normalized in such a way as to make the two functions numerically equal in this voltage range.

plotted on a semi-logarithmic scale as a function of time. The values of τ_{AK} and τ_{BK} obtained in this way are shown in Fig. 4 (open circles). By extrapolating the separated components $A_K(V, t)$ and $B_K(V, t)$ back to zero time (point at which post-spike clamp was instituted), one finds, up to an arbitrary multiplicative constant, $B_K(V, \infty)$; these values are shown in Fig. 5.

By considering the conductances over a wider range of voltages, it is possible to extend the preceding analysis to give the time constants and steady-state values shown in Figs. 4 and 5. Fig. 6 presents g_K variations

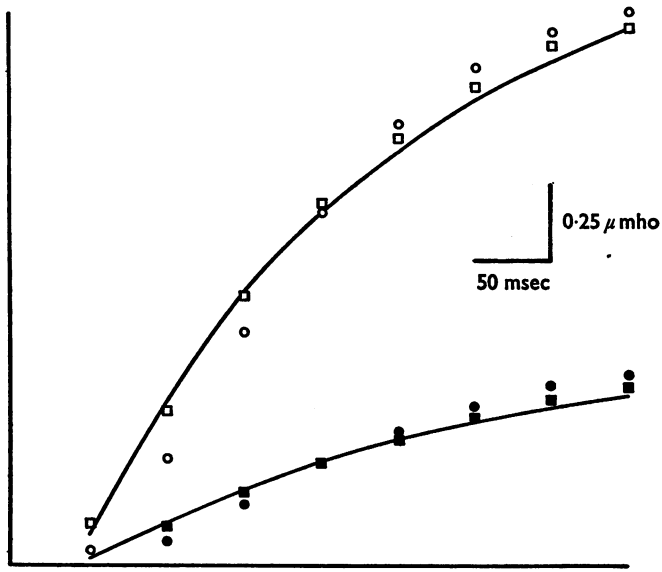

Fig. 6. Continuous traces: activation of g_K associated with membrane voltage steps from -40 to -10 mV (upper trace) and from -40 to -18 mV (lower trace). Squares: fit achieved by two time constant approximation described in text. Circles: fit achieved by fourth power of simple exponential (Hodgkin–Huxley approximation). The initial part of the curves is contaminated by inward current and is not considered in these two cases.

produced by a depolarizing clamp, and gives the predicted values from eqns. (6) and (7), and the parameters in Figs. 4 and 5. It is apparent that the fit is adequate but not perfect. In Fig. 7*A* a family of clamping currents following action potentials is shown, and with it, the predicted values from eqns. (6) and (7). For comparison, the conductances predicted by equations of the same form used by Hodgkin & Huxley for their potassium conductances are shown in Figs. 6 and 7*B*.

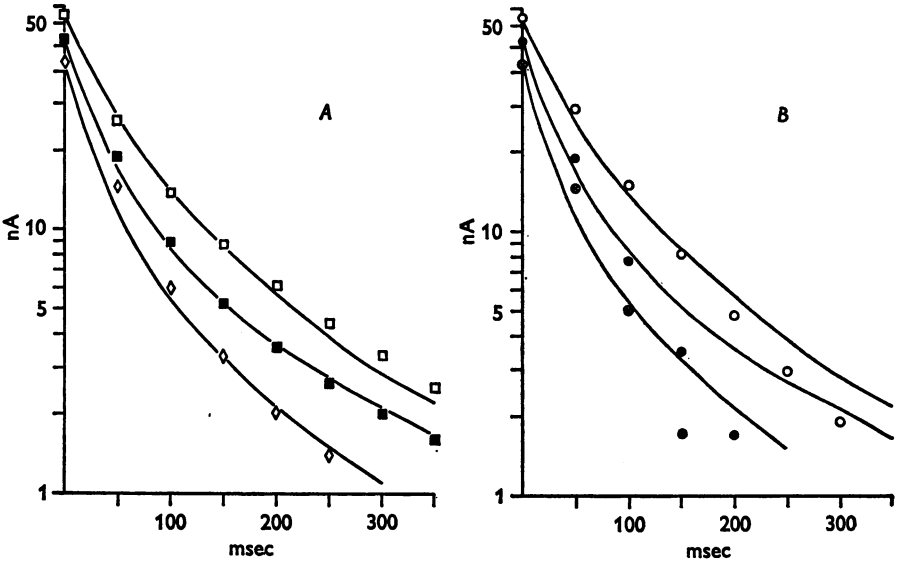

Fig. 7. *A*. Continuous curves: transient part of currents (total current minus steady-state current) associated with post-spike clamping voltages of −29 mV (top curve), −34·5 mV (middle curve), and −38 mV (bottom curve). Symbols show fit achieved by the two time constant model described in text. *B*. Same currents as in part *A*. Symbols show fit achieved by fourth power of simple exponential.

SECTION 2

The complete set of descriptive equations is summarized in (9).

$$\left.\begin{aligned} I(t) &= C\frac{dV}{dt} + \sum_{j=1}^{4} \bar{g}_j A_j^j (V,t)\, B_j (V,t)\,(V - V_j), \\ \tau_{Aj}(V)\frac{dA_j(V,t)}{dt} + A_j(v,t) &= A_j(V,\infty), \\ \tau_{Bj}(V)\frac{dB_j(V,t)}{dt} + B_j(V,t) &= B_j(V,\infty). \end{aligned}\right\} \quad (9)$$

The values for the various parameters are specified in Table 1 for the exemplar cell.

If the analysis embodied in equations grouped as (9) is correct, the solution to these equations should successfully predict membrane potential for any applied current. Approximate solutions to (9) for a number of stimulus conditions have been obtained, and in general they do yield accurate predictions; the extent of agreement between observed and predicted membrane potential, and the deficiencies in these predictions will now be described.

If eqns. (9) are solved for applied current equal to zero, the observed resting potential of -40 mV is accurately predicted. Solutions for a wide range of depolarizing currents yield infinite trains of spikes at a frequency which depends upon stimulus intensity. For at least a sevenfold range of stimulus intensities, reciprocal interspike interval, that is, impulse frequency, is linearly related to applied current, and for larger stimulating currents, saturation occurs so that frequency increases less rapidly with further increments in stimulus intensity. The predicted curve for impulse frequency as a function of stimulating current intensity is given in Fig. 8 (filled circles), and in the same Figure the observed values for the

TABLE 1. Parameters of eqns. (9) for the exemplar cell. Straight-line approximations in cited figures were used in computations. $C = 14$ pF

j	Letter designation	τ_{Aj} (V)	τ_{Bj} (V)	$\bar{g}_j A_j^i (V, \infty)$	$B_j (V, \infty)$	V_j
1	L	0	0	0·049 μmho	1	-40 mV
2	K	Fig. 4	Fig. 4	Fig. 5	Fig. 5	-60 mV
3	I	Fig. 1	Fig. 1	21 μmho times values in Fig. 2	Fig. 2	$+45$ mV
4	A	12 msec	235 msec	Fig. 3	Fig. 3	-63 mV

reciprocal of the exemplar cell's first interspike interval are plotted. When these predictions were carried out, a slight error was present in the steady-state $A_I (V, \infty)$ curve (see Fig. 2), so that inward current increased too rapidly with depolarizations and caused the predicted action potentials to occur slightly too early; this error in estimating the inward current mechanism accounts for the fact that all of the predicted frequencies are slightly too large, but the error was not large enough to require the calculations to be repeated with the more accurate value for $A_I (V, \infty)$. It is apparent that the observed and predicted frequencies agree quite well not only in the linear region, but also for higher stimulus intensities where saturation is occurring.

For a step of depolarizing currents, eqns. (9) predict that the membrane potential rises approximately linearly to about -25 mV, and then curves sharply up into an action potential whose peak reaches $+25$ mV and whose duration is about 25 msec. After the action potential there is a hyperpolarization and then an approximately linear rise again to a second spike. Observed and predicted membrane potentials are shown in Fig. 9*A* and *B* (on a slower time base). Although the observed and predicted curves in Fig. 9*A* are quite close, the depolarization in the predicted curve develops more slowly and the predicted spike occurs later. These differ-

ences are within the range of experimental error (small changes in stimulus intensity and membrane capacitance would bring the observed and predicted curves into closer agreement) but we feel the disagreement is in fact primarily the result of inaccuracies in the inward current mechanism description; these will be discussed later. On the slower time base of Fig. 9*B*, the observed and predicted membrane potential trajectories are again in quite close agreement. The downswing of the predicted action potential is not quite rapid enough, a deficiency we attribute to insufficient activation of g_K.

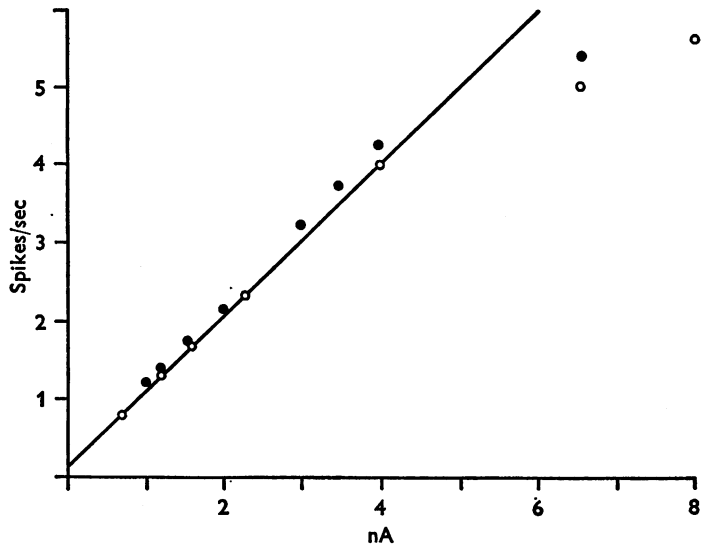

Fig. 8. Firing frequency (ordinate) plotted against transmembrane stimulus current (abscissa) for exemplar cell (open circles) and model (filled circles).

To the extent that our analysis is indeed accurate, it is now possible to understand the role each conductance plays in determining membrane potential during repetitive firing. When current is first applied, the membrane starts to depolarize, but as it does so g_A is activated and an outward potassium current flows which opposes the applied current, thus slowing the rate of depolarization. The interaction of the g_A activation and the charging of the membrane capacitance by the applied currents causes membrane potential to increase approximately linearly to the voltage where g_I becomes more rapidly activated. As current flows through g_I, the cell becomes rapidly depolarized and the spikes ensue. During the upswing of the spike the inward current channels become inactivated and the potassium channels become activated, until at the peak of the spike the potassium and inward current are equal. After this point, the potassium

current exceeds the inward current, which is now almost completely inactivated, and the membrane potential is rapidly returned toward the resting potential. The large potassium conductance resulting from the spike hyperpolarizes the cell and dominates behaviour during the first part of the interspike interval. As g_K decreases toward its resting value, the membrane starts depolarizing under the influence of the applied currents. However, the g_A channels have lost some of their inactivation during the period of hyperpolarization, and as the membrane depolarizes these

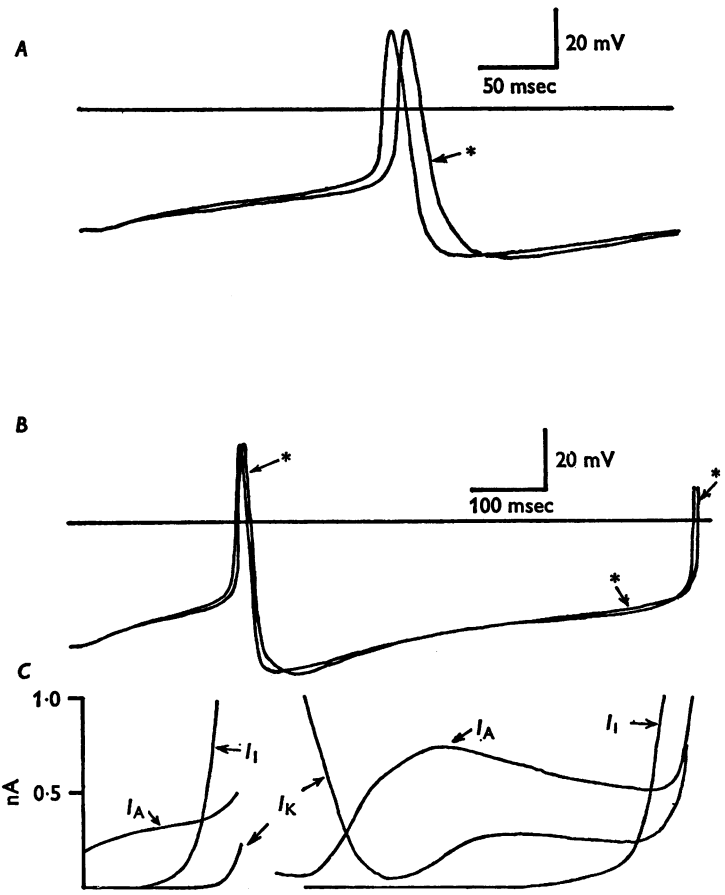

Fig. 9. *A*. Comparison of an action potential recorded from the exemplar cell and a computed action potential. Computed A.P. indicated by (*). *B*. Computed (*) and recorded action potentials at compressed time scale for comparison of membrane voltage behaviour between A.P.s. Stimulus current, 1·6 nA. *C*. Computed membrane currents associated with the computed voltage behaviour of part *B*. Currents flowing during the action potentials are not shown because their large magnitude would obscure subthreshold behaviour.

channels are activated, and slow the rate of depolarization by opposing the applied current with a potassium current. Toward the end of the interval the inward current mechanism is slowly activated, so that, finally, a balance of inward and outward currents is achieved through the g_I and g_A channels, and a linear rise in membrane potential results. At a sufficient depolarization, the inward current mechanism dominates and another spike ensues. This sequence of events is illustrated in Fig. 9*C*.

Because the conductance g_A is not present in the more thoroughly analysed squid axon and frog node, it is of interest to consider situations which make the action of this mechanism most prominent. At -40 mV, g_A is largely inactivated (see Fig. 3), so a prolonged hyperpolarizing pulse should remove this inactivation and place the membrane in a state where, on depolarization, the effects of g_A would be most strongly felt. In Fig. 10*A*, the membrane potential recorded from a second neurone on which analysis was performed is shown. The cell was subjected to a 500 msec hyperpolarizing current (Fig. 10*C*) followed by a depolarizing current. When the depolarizing stimulus is applied the membrane potential rises rapidly, overshoots, and then proceeds smoothly toward the takeoff of the action potential. This behaviour is the consequence of removal of inactivation from g_A by the hyperpolarization, followed by the activation and inactivation of g_A. The open circles in Fig. 10*A* show the predicted response up to the spike take-off and indicate satisfactory agreement between observed and predicted membrane potentials. Thus, the behaviour of the membrane after a prolonged hyperpolarization is dominated by the properties of g_A. Two other effects of g_A, not illustrated in the Figure, are the following: first, with a pre-spike membrane potential more negative than about -50 mV, the membrane potential rises very slowly to the point where the first action potential is initiated. This effect is the result of large I_A currents which develop because of relatively small initial inactivation at the resting potential. This current cancels applied current, and in effect makes even large stimulus intensities result in only slowly increasing depolarizations. This situation is the normal one for most unligated cells. Because the exemplar cell soma was isolated and had a resting potential of only -40 mV, the effect could be achieved only by pre-hyperpolarization. A second effect, seen in many preparations, is that the first interspike interval of a train following a hyperpolarization is longer than would ordinarily be observed. This abnormally long first interval results because the g_A inactivation has not, by the time an action potential has occurred, developed to its steady-state level, and so the effect of g_A is more prominent than normal during the first interspike interval. Thus, the I_A currents retard the rate of interspike depolarization and prolong the interval. This effect can persist over several intervals if the firing

frequency is high enough to permit several spikes to fire before B_A has reached a steady-state level. The effects just described are adequately predicted by eqns. (9).

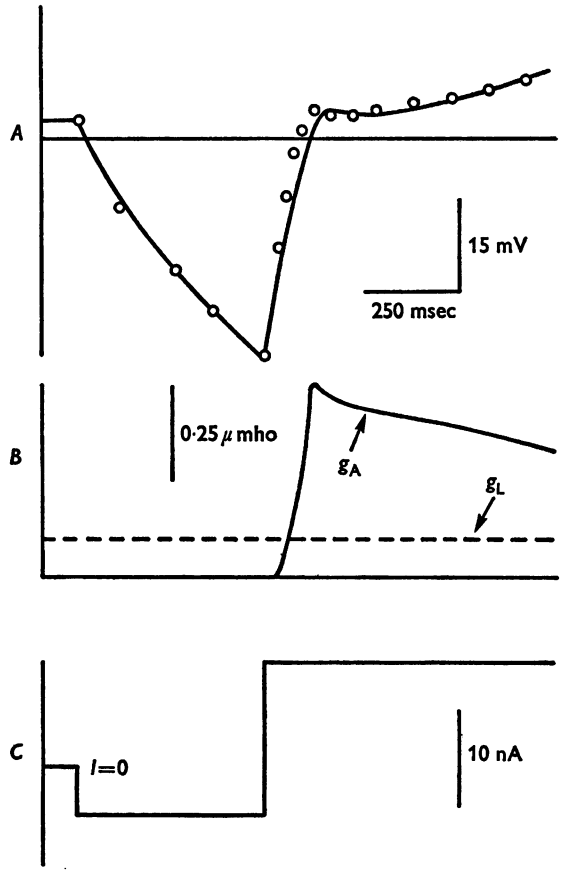

Fig. 10. *A*. Recorded membrane voltage (continuous line) and computed response (circles) to the current stimulus shown in part *C*. *B*. Computed behaviour of g_A associated with voltage changes of part *A*. Leakage conductance, g_L, is indicated by dashed line. g_i and g_K are negligible for voltages in the range shown. $V_L = -42$ mV. $V_A = -63$ mV.

The preceding description of the mechanisms controlling membrane potential during the interspike interval holds for the range of frequencies into the saturation region. For very high frequencies, however, the cell membrane fails to repolarize to sufficiently negative values after a spike for g_A to lose its inactivation. In these cases, g_A plays no role in repetitive firing, and membrane potential is determined solely by the other conductances.

DISCUSSION

The properties of g_I are difficult to measure with accuracy because separation of I_I and I_K is difficult, and because the activation of g_I is too rapid to be well resolved with the voltage clamping system employed in these experiments. Nevertheless, the analysis of g_I is sufficiently accurate to yield relatively good predictions for the action potential as seen in Fig. 9*A*. The most serious difficulty with the description of the inward current mechanism appears to involve the inactivation term $B_I(V, t)$. The second and succeeding computed spikes in long trains are approximately 5 mV smaller than the first spike, an occurrence seldom seen in preparations. Furthermore, a long, maintained depolarization before the first spike also can give rise to a predicted action potential which is smaller than that observed in the preparation. Although the effect has not been analysed, in several experiments there has appeared what must be an inactivation process affecting g_I with a time constant on the order of 400 msec. The steady-state inactivation curve used for the computations (Fig. 2*A*) was obtained in a manner which would include both the rapid and the slower types of inactivation. Thus inactivation, which should partly develop with a slow time course, reaches its steady-state rapidly in our equations, and thus for slowly increasing depolarizations there is a tendency for the inactivation to be larger than it should be. This effect must be analysed in greater detail before completely satisfactory predictions of repetitive firing can be made.

The analysis of g_K is difficult primarily because the large currents which flow with large depolarizations appear to cause potassium accumulation in the Frankenhaeuser–Hodgkin space (Frankenhaeuser & Hodgkin, 1956), and thus give a non-constant equilibrium potential for the process. Furthermore, cells seem to deteriorate rapidly when a series of very large depolarizations is used. It is, of course, difficult to analyse g_K accurately without the benefit of accurate data over a wide range of membrane potentials. Thus, we have concentrated on obtaining a thorough description for the range of membrane potentials below -30 mV. Furthermore, since our interest has been processes which are rapid compared to the potassium inactivation, that factor has not been included in the equations. For technical reasons, then, the analysis of g_K has certain limitations. Beyond this, however, the behaviour of these channels seems quite complicated, and thus yields less readily to analysis than, for example, the conductance, g_A. We have departed from the Hodgkin–Huxley fourth power analysis of g_K because this description seemed not sufficiently accurate, and furthermore, because certain qualitative observations point to the existence of two separate processes (termed $A_K(V, t)$ and $B_K(V, t)$). The

most striking of these is the behaviour of g_K that is seen when a clamp is instituted above -20 mV after a spike has been elicited (see Connor & Stevens, 1971*a*; Fig. 9). In this case, the currents decreased and then after a dip increased to their steady level. Such behaviour cannot be exhibited by the traditional g_K description, but is readily modelled by the two separate processes as done here. The physical meaning of these processes remains obscure, and we cannot even be confident that this behaviour is not the result of two separate mechanisms, a traditional g_K, and a chloride conductance, for example. A second deficiency in the description of repetitive firing given here, then, is the incomplete analysis of the g_K mechanism.

The model presented gives, except under special circumstances described below, infinite trains of action potentials with a constant interspike interval; that is, the first and each succeeding interval are all of the same length. The preparation, on the other hand, almost always shows a lengthening of interspike interval as the train proceeds. Thus, the model predicts a constant impulse frequency to a steep stimulation, whereas the actual preparation shows a frequency which decreases somewhat when step stimulation is employed. The predictions in the paper were compared with the first interspike interval and are reasonably accurate. For subsequent intervals, the model predicts a firing rate which is too high. This phenomenon has not yet been analysed in detail but some preliminary experiments, in which a clamp was instituted following a train of spikes, have indicated that, associated with such a train, there is an increase in potassium conductance which decays with a time course much slower than any described for g_K in the paper. Such a long time constant potassium mechanism could, of course, account for the adaptation exhibited by the preparation but absent in our description of repetitive firing. Such a conclusion must, however, await further experimental data.

The preliminary evidence just mentioned suggests the existence of a slow potassium system in the preparation, and thus, the description given here is inaccurate to the extent that such a conductance is important in repetitive firing. Two other phenomena are also present in these neurones, neither is included in the preceding description, and for neither has the role in repetitive discharge been adequately evaluated. Potassium inactivation is certainly present (Connor & Stevens, 1971*a*), and in fact, can be quite marked. This was not included in the model, and the functional significance of this process remains obscure. Although the electrogenic sodium pump (Connelly, 1959; Nakajima & Takahashi, 1966; Carpenter & Alving, 1968; Thomas, 1969) present in these cells does not fit into the framework of the present analysis in terms of conductances, this phenomenon should affect the cell's behaviour in that pumping rate might

increase with cellular activity. The magnitude of this effect must be evaluated experimentally, and because our experiments were typically done at low temperatures where electrogenic sodium pump activity is depressed, we have no information on its role in the phenomenon of repetitive firing.

The conductance termed g_A has been seen to dominate the behaviour of the cell in certain circumstances. It is of interest to know if the presence of such a mechanism can be detected in other neurones without the necessity of carrying out voltage clamp experiments. Two phenomena which depend on g_A, both present in the observed and predicted behaviour of these neurones, can serve as tests for the presence of g_A. If a neurone is hyperpolarized and then depolarized, the characteristic overshooting behaviour illustrated in Fig. 9 results from g_A, and offers the possibility of detecting the presence of this mechanism when only current clamp is available. Secondly, if a depolarizing stimulus is preceded by a long-lasting and large hyperpolarizing stimulus, the first interspike interval is longer than it would have been had the depolarizing stimulus been employed without prior hyperpolarization. This effect too should reveal the presence of g_A. It must be emphasized, however, that both of these effects depend on the time constants of g_A relative to the membrane time constant and to the period between the spikes. Thus, to detect g_A by the presence of a longer first interspike interval, it is required that the interspike interval be comparable to the time constant for g_A inactivation; higher stimulus intensities then yield a more sensitive test than do low stimulus intensities which give long interspike intervals. It will be interesting to see if other neurones, particularly those in the central nervous system, share this property with the molluscan neurones we have studied.

Although the analysis we have presented here is not complete in all respects, we feel that the satisfactory agreement between predicted and observed neuronal behaviour indicates that the primary processes underlying the phenomenon of repetitive firing have been revealed, and that we have given an essentially correct description of the control of membrane potential during the interspike interval in the preparation studied. We hope that this work will serve as a useful foundation for further investigations of repetitive discharge in the isolated neurone soma, and for an analysis of this phenomenon in the vertebrate central nervous system.

We wish to thank Professor Theodore Kehl for making available to us the computer facilities he directs and for advice in computer applications. We are also indebted to Tina Moss for help in programming. This research was supported by USPHS Grants NB 06934, NB 05082 and FR 00374.

REFERENCES

CARPENTER, D. O. & ALVING, B. (1968). A contribution of an electrogenic Na^+ pump to membrane potential in *Aplysia* neurons. *J. gen. Physiol.* **52**, 1–21.

CONNELLY, C. M. (1959). Recovery processes and metabolism of nerve. *Rev. mod. Phys.* **31**, 475–484.

CONNOR, J. A. & STEVENS, C. F. (1971*a*). Inward and delayed outward membrane currents in isolated neural somata under voltage clamp. *J. Physiol.* **213**, 1–19.

CONNOR, J. A. & STEVENS, C. F. (1971*b*). Voltage clamp studies of a transient outward membrane current in gastropod neural somata. *J. Physiol.* **213**, 21–30.

DODGE, F. A. & FRANKENHAEUSER, B. (1959). Sodium currents in the myelinated nerve fibre of *Xenopus laevis* investigated with the voltage clamp technique. *J. Physiol.* **148**, 188–200.

FRANKENHAEUSER, B. & HODGKIN, A. L. (1956). The after-effects of impulses in the giant nerve fibres of *Loligo*. *J. Physiol.* **131**, 341–376.

FRANKENHAEUSER, B. & HUXLEY, A. F. (1964). The action potential in the myelinated nerve fibre of *Xenopus laevis* as computed on the basis of voltage clamp data. *J. Physiol.* **171**, 302–315.

HODGKIN, A. L. & HUXLEY, A. F. (1952). A quantitative description of membrane current and its application to conduction and excitation in nerve. *J. Physiol.* **117**, 500–544.

NAKAJIMA, S. & TAKAHASHI, K. (1966). Post-tetanic hyperpolarization and electrogenic Na pump in stretch receptor neurone of crayfish. *J. Physiol.* **187**, 105–127.

NOBLE, D. & TSIEN, R. W. (1969*a*). Outward membrane currents activated in the plateau range of potentials in cardiac Purkinje fibres. *J. Physiol.* **200**, 205–231.

NOBLE, D. & TSIEN, R. W. (1969*b*). Reconstruction of the repolarization process in cardiac Purkinje fibres based on voltage clamp measurements of membrane currents. *J. Physiol.* **200**, 233–254.

OCHS, A. L. (1967). Changes in membrane properties with hyperpolarization in snail neurons. *Am. J. Physiol.* **231**, 16–20.

THOMAS, R. C. (1969). Membrane current and intracellular sodium changes in a snail neurone during extrusion of injected sodium. *J. Physiol.* **201**, 495–514.